Divergent pathways of cyclonic and anti-cyclonic ocean eddies

R. Morrow, F. Birol, D. Griffin, J. Sudre

▶ **To cite this version:**

R. Morrow, F. Birol, D. Griffin, J. Sudre. Divergent pathways of cyclonic and anti-cyclonic ocean eddies. Geophysical Research Letters, 2004, 31 (24), pp.ISI:000226133200004. 10.1029/2004GL020974 . hal-00434484

HAL Id: hal-00434484
https://hal.science/hal-00434484

Submitted on 22 Feb 2021

HAL is a multi-disciplinary open access archive for the deposit and dissemination of scientific research documents, whether they are published or not. The documents may come from teaching and research institutions in France or abroad, or from public or private research centers.

L'archive ouverte pluridisciplinaire **HAL**, est destinée au dépôt et à la diffusion de documents scientifiques de niveau recherche, publiés ou non, émanant des établissements d'enseignement et de recherche français ou étrangers, des laboratoires publics ou privés.

Divergent pathways of cyclonic and anti-cyclonic ocean eddies

Rosemary Morrow and Florence Birol
Laboratoire d'Etudes en Géophysique et Océanographie Spatiales, Toulouse, France

David Griffin
Commonwealth Scientific and Industrial Research Organization Marine Research, Hobart, Tasmania, Australia

Joël Sudre
Laboratoire d'Etudes en Géophysique et Océanographie Spatiales, Toulouse, France

Received 9 July 2004; revised 14 October 2004; accepted 9 November 2004; published 30 December 2004.

[1] Satellite altimetry is used to study the propagation pathways of warm and cold ocean eddies in different ocean basins. We consider eddies that have a life span longer than 3 months, and we present three regional studies: in the southeast Indian, the southeast Atlantic, and the northeast Pacific Oceans. The case studies show that simple theories for vortex propagation on a β-plane work in regions where energetic eddies propagate though a weak background flow. Under these conditions, anticyclonic/cyclonic eddies propagate westward and equatorward/poleward. This divergence in the eddy pathways implies a net equatorward eddy heat flux, and has implications for the meridional transport of freshwater, carbon, nutrients, etc. *INDEX TERMS:* 4520 Oceanography: Physical: Eddies and mesoscale processes; 4516 Oceanography: Physical: Eastern boundary currents; 4275 Oceanography: General: Remote sensing and electromagnetic processes (0689). **Citation:** Morrow, R., F. Birol, D. Griffin, and J. Sudre (2004), Divergent pathways of cyclonic and anti-cyclonic ocean eddies, *Geophys. Res. Lett.*, *31*, L24311, doi:10.1029/2004GL020974.

1. Introduction

[2] Propagating Rossby waves play an important role in transferring energy across the ocean basins, and also interact dynamically with western boundary currents. Ocean eddies or vortices can transfer heat, salt, carbon, nutrients, and other tracers across the ocean [*Morrow et al.*, 2003] and act to accelerate and transfer energy to the mean currents. So monitoring their propagation pathways, evolution and decay is important to understand their role in the global tracer budgets.

[3] Satellite altimetry is a robust way of tracking propagating features because the sea level anomalies are a depth-integrated response: we continue to track the deeper signal of these planetary waves and ocean eddies long after their surface mixed layer has been modified by seasonal forcing. The precise Topex/Poseidon data have provided an unprecedented view of the global ocean Rossby wave field, their time and spatial scales and their westward propagation speeds [*Chelton and Schlax*, 1996]. Mid-latitude ocean eddies are also detected with satellite altimetry [*Le Traon and Morrow*, 2001], and their space-time sampling is improved using a combination of different altimeters [*Le Traon et al.*, 1997].

Copyright 2004 by the American Geophysical Union.
0094-8276/04/2004GL020974

[4] Although the zonal propagation of oceanic Rossby waves and mesoscale eddies has been well documented (e.g., mapped with Hovmuller diagrams along different latitude bands) only a few investigations have addressed their meridional propagation. The statistics of the meridional propagation of North Atlantic Rossby waves have been described by *Challenor et al.* [2001] and the meridional propagation of ocean vortices have been investigated theoretically and numerically by *Cushman-Roisin et al.* [1990] and *Chassignet and Cushman-Roisin* [1991]. When tracking individual ocean eddies, certain meridional patterns have been revealed. For example, large, warm, anticyclonic Agulhas rings pinching off from the Retroflection region propagate WNW into the south Atlantic Ocean whereas cyclonic eddies propagate WSW [*Boebel et al.*, 2003]. In the southeast Indian Ocean, warm, anticyclonic eddies separating from the coastal Leeuwin Current propagate WNW over the Perth Basin, and then follow a more zonal route [*Fang and Morrow*, 2003], whereas a cold eddy with an entrapped drifter was observed to travel to the WSW [*Griffin et al.*, 2001]. In the Southern Ocean south of Tasmania, cold, cyclonic eddies generated over a bathymetric rise tend to propagate WSW [*Morrow et al.*, 2004]. These intriguing patterns led us to undertake a more systematic study of the propagation pathways of warm and cold ocean eddies in different ocean basins.

2. Data and Methods

2.1. Altimetric Sea Level Anomaly Data

[5] Five years of altimetric sea level anomaly (SLA) data (1996–2000) used in this study are based on the gridded Topex/Poseidon (T/P) and ERS1-2 SLA data distributed by CLS-Space Oceanography Division [*Le Traon et al.*, 1997]. The 1/3° gridded data set provides the best available spatial-temporal resolution for observing mesoscale features, particularly in the mid to high-latitude regions where the first internal Rossby radius is of order 30–50 km. The gridded data resolved 100 km wavelength signals; variations at 50 km wavelength have their energy reduced by 50% [*Ducet et al.*, 2000].

2.2. Detecting and Monitoring Ocean Eddies

[6] Our main problem is how to systematically identify individual mesoscale ocean eddies from a series of altimetric SLA maps. Following *Isern-Fontanet et al.* [2003], we define the eddy cores as regions in which the second

Table 1. Values Applied for the Selection Criteria in the Three Study Regions

Region	SE Indian		SE Atlantic		NE Pacific	
Rotation	A/C	Cyc	A/C	Cyc	A/C	Cyc
Q_0 (10^{-11} s^{-2})	1		2.5		1	
H_0 (cm)	20	−20	30	−25	8	−8

invariant of the velocity gradient tensor is positive. We can express this in terms of a parameter, Q:

$$Q = -\left(\frac{\partial u}{\partial x}\right)^2 - \left(\frac{\partial v}{\partial x}\right)\left(\frac{\partial u}{\partial y}\right) > 0,$$

which is based on the 2D velocity field, (u, v) derived from the altimeter SLA maps assuming the geostrophic approximation. Assuming that the vorticity and the strain are slowly varying with respect to the vorticity gradient along a particle path, the term Q measures the relative contribution of the flow rotation and its deformation. For $Q > 0$, the rotation dominates the deformation. A vortex exists in regions where Q is positive and relatively large, $Q > Q_0$. In our case studies, we tested various threshold values for Q_0, and selected Q_0 as $2 \times 10^{-11}s^{-1}$ in the Agulhas region where the eddy energy is high, and $1 \times 10^{-11}s^{-1}$ elsewhere. Initial tests in the southeast Indian Ocean revealed a large number of eddies were selected using the $Q > Q_0$ criterion, especially near the coast and in regions of low eddy energy where the signal-to-noise ratio is low. In order to select the larger amplitude, long-lived eddies, we added a criterion that SLA > H_0 for anticyclonic eddies, SLA < H_0 for cyclonic eddies. The eddy lifetime is >90 days and >120 days in the Agulhas. The final values for Q_0 and H_0 are summarized in Table 1 for each of our three case studies.

[7] We developed an automatic tracking technique to monitor the eddy propagation. All eddies with $Q > Q_0$ and $|SLA| > H_0$ are identified in the initial map at time, t_0. We then search for the same eddy structure within a spatial radius, R, around our initial eddy position in the next map at time t_0 + 10 days. Since the propagation speed of these mid latitude eddies is a few km per day, the search radius R is set at 1°. We also identify new eddies in each new map. Sometimes the eddy structures weaken or disappear between consecutive maps if they pass into the gaps between satellite groundtracks. To minimize this problem, we keep searching for the same eddy for 20 days after it "disappears".

3. Observed Eddy Propagations

3.1. SE Indian/Leeuwin Current Eddies

[8] The propagation pathways for anti-cyclonic and cyclonic eddies is shown in Figure 1 for the southeast Indian Ocean. The warm eddy propagation has been described by *Fang and Morrow* [2003]. The distribution of long-lived, warm eddies is concentrated near the coast and north of 35°S. South of 25°S, 74% of the warm eddies tend WNW as they pass across the Perth Basin and are then channeled around the bathymetry west of 105°E. Their mean westward speed if 2.6 km/day, with a weak equatorward speed of 0.4 km/day. North of 25°S, their propagation is mainly zonal, and the SLA signal is dominated by Rossby waves [*Birol and Morrow*, 2003]. Their relative vorticity increases towards higher latitudes for two reasons. Firstly, the Rossby radius decreases so the spatial gradients in the velocity field are confined to a smaller radius. Secondly, there is an increase in SLA with latitude [*Fang and Morrow*, 2003] which has a direct effect on the relative vorticity. Part of the eddy field is spawned from instabilities of the Leeuwin Current which brings warm, low salinity water poleward creating large positive SLAs with respect to the progressively cooler offshore water. Relative vorticity also tends to decrease offshore, probably related to the observed decay in SLA over time [*Fang and Morrow*, 2003].

[9] Cyclonic propagation is more distinctive; 84% show a clear poleward propagation, with faster meridional speeds (mean of 0.8 km/day) than for the anticyclones. The distribution of cold eddies is concentrated further offshore and south of 27°S. Their relative vorticity increases towards higher latitudes at the coast, but there are only minor changes in their relative vorticity values over time, as these eddies propagate WSW.

3.2. Southeast Atlantic/Agulhas Eddies

[10] Figure 2 shows the propagation pathways for warm and cold eddies in the south Atlantic region west of the Agulhas Retroflection. The behavior of the long-lived warm Agulhas rings and their general westward and equatorward propagation, bringing warm high salinity water from the Indian to the south Atlantic, has been described by many

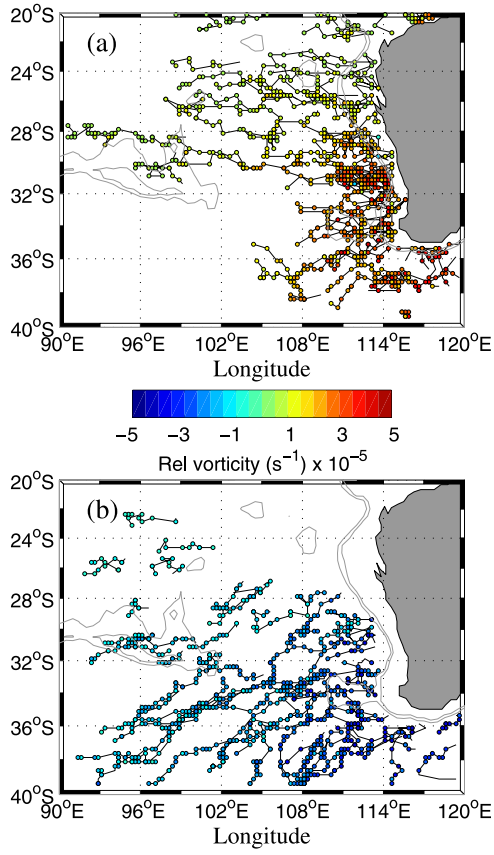

Figure 1. Propagation pathways for anti−cyclonic eddies (upper panel) and cyclonic eddies (lower panels), in the southeast Indian Ocean. Their relative vorticity is represented by the colored circle: one every 10 days along their pathway.

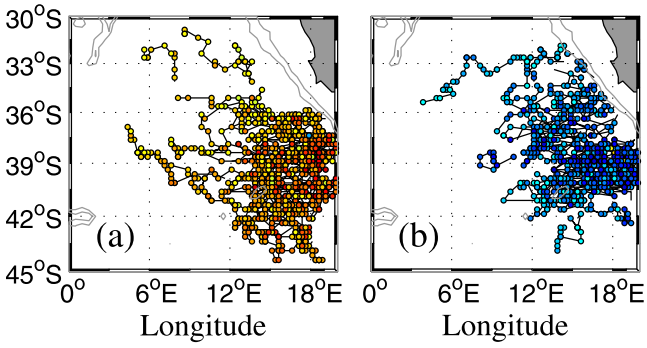

Figure 2. As for Figure 1, but in the southeast Atlantic Ocean. Color bar shown in Figure 1.

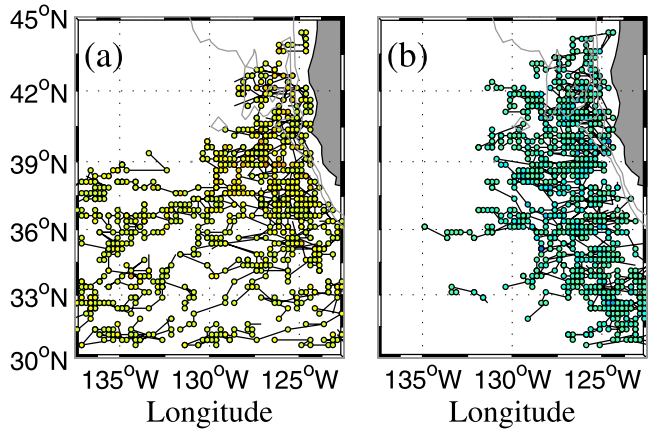

Figure 3. As for Figure 1, but in the northeast Pacific Ocean. Here we plot negative relative vorticity for this northern hemisphere case, so that anti−cyclonic eddies remain in yellow/red, and cyclonic eddies in blue.

authors (see *de Ruijter et al.* [1999] for a review). The highly energetic region from 12−20°E, 35−44°S known as the "Cape Cauldron", is one of vigorous mixing and strong cyclonic and anti-cyclonic interactions [*Boebel et al.*, 2003] evident in the complex propagation pathways. The largest relative vorticity values are located in the Cauldron where the SLAs are the highest in the world. Farther west and north, we observe lower, stable relative vorticity, with little decay in relative vorticity along the cyclonic or anticyclonic pathways, and the divergence in eddy pathways becomes more apparent. We find 65% of the anticyclones propagate equatorward with meridional speeds around 0.2 km/day and 66% of the cyclones propagate poleward at 0.3 km/day. *Boebel et al.* [2003] also studied cyclonic versus anticyclonic propagation using altimetry and RAFOS floats from 1997−1999, using a different tracking criteria. They identified 43 cyclones, with a mean poleward propagation of 0.3 km/day, with fewer, larger anticyclones (29) with a mean equatorward speed of 1.1 km/day. The different selection criteria and time periods of the two studies lead to slightly different propagation statistics, but both show consistent divergence in the eddy pathways.

3.3. NE Pacific/Californian Current Eddies

[11] Figure 3 shows the propagation pathways in the northeast Pacific Ocean just offshore from the Californian Current. The eddy kinetic energy is much lower in comparison to the southeast Indian or southeast Atlantic, so our SLA H_0 criterion was reduced to an 8 cm level. Both warm and cold eddies are present in the coastal band, but the cold eddies decay below the 8 cm level within 1000 km of the coast, with no clear poleward propagation. In contrast, the warm eddies have a longer lifespan, propagate much farther west, and 60% have a clear equatorward propagation at 0.4 km/day. Neither the warm or cold eddies show any real changes in their relative vorticity field over time. We note that our analysis period includes the very strong El Nino event which increased the upper ocean temperature along the west coast of the from late 1997 through to late 1998. So the large number of long-lived warm eddies in our analysis may be influenced by this event, and the distribution of eddies may be different during other time periods.

4. Discussion

[12] What causes this divergence in the warm and cold eddy pathways? These eddies are relatively large with diameters >100 km (the mapping technique smooths out the smaller-scale eddies). Being large, the β-effect can influence their rotation. As the eddies rotate they generate an advection of the surrounding fluid in the same direction: the surrounding fluid changes latitude and planetary vorticity, f, which induces small anticyclonic and cyclonic vorticies on the flanks of the large vortex. These small secondary vorticies combine with the large vortex to cause the meridional drift. Figure 4, after *Cushman-Roisin* [1994], shows how the different sign of relative vorticity on each flank of the eddy pushes a cyclonic eddy poleward, and an anticyclonic eddy equatorward.

[13] As the vortex moves meridionally, its own core undergoes a change in planetary vorticity, in the sense to reduce the absolute value of its core relative vorticity. This reduction in relative vorticity along the eddy pathway has been observed for warm eddies in the Leeuwin Current as they decay during the first 3 months, but is only minor for our other case studies. In general, the observed eddies maintain their SLA and near constant core relative vorticity over many years.

[14] Why don't we see this divergence near the eddy-rich western boundary currents or near zonal currents such as the Antarctic Circumpolar Current or the Azores Current? Instabilities from a near zonal flow will generate anticyclonic/cyclonic eddies on the poleward/equatorward side, which then drift back and are quickly reabsorbed by the mean jet. In contrast, cyclonic and anticyclonic eddies

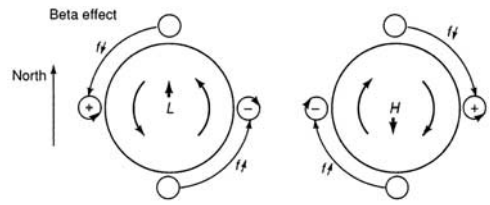

Figure 4. Meridional drift of vorticies on a β-plane [after *Cushman-Roisin*, 1994]. The figure is drawn for the Northern Hemisphere, in the Southern Hemisphere cyclones still move poleward and anticyclones equatorward.

generated by a meridional eastern boundary current propagate westward offshore and are then free to follow their destiny: cyclones towards the poles and anticyclones towards the equator. The divergence of the cyclonic/anticyclonic eddies is also noted on the western flank of large bathymetric features, such as the south Tasman Rise [*Morrow et al.*, 2004] and off the Hawaiian Islands (S. Imawaki, personal communication, 2004).

[15] However, our three eastern boundary cases show very different divergence patterns. The California Current eddies have fairly low energy, so we cant track them for long, and the results are not very conclusive. The Leeuwin Current and Agulhas eddies are more energetic and coherent, so we can track their propagation pathways longer. The Agulhas eddies traverse a region with large bathymetric features and relatively strong background flow, both of which can perturb the propagation pathways. Whereas the Leewin Current eddies traverse a wide deep basin with weak background flow, closer to the ''ideal'' theoretical case. This may explain the distinct divergence pattern of the southeast Indian Ocean, though more investigation of their different dynamics is required.

[16] One of the most interesting aspects of this systematic divergence is its potential effect on global tracer budgets and on the meridional transport of different tracers (heat, salt, carbon, nutrients, etc). For example in the southeast Indian Ocean, there is a clear population of warm eddies moving equatorward and then zonally across the band 20–30°S, and cold eddies moving equatorward and occupying the offshore region from 30–40°S. This spatial pattern coincides exactly with the pattern of net heat flux to the atmosphere [*Josey et al.*, 1999] which is anomalously negative (ocean heat loss) over the region occupied by the warm eddies and positive (ocean heat gain) over cold eddy region. The pattern of surface heat loss/gain extends far into the ocean interior, and the long-lived eddies arriving here have undergone many seasonal cycles. However, regions with a large population of warm eddies with deep thermoclines could maintain a surface heat storage over many years. In contrast, the region to the south with cold eddies, and a raised thermocline, can maintain a source of cool, deeper water close to the surface. More quantitative studies on the air-sea exchanges in these two zones are required, but we note that the cold eddies enter a region of very deep winter mixed layers where the southeast Indian Subantarctic Mode Water forms [*McCartney*, 1982]. Perhaps the large population of cold eddies helps to precondition the deep winter convection?

[17] The divergence of the warm and cold eddies could also lead to a net equatorward heat transport in these eastern boundary regions (anticyclones/cyclones transporting positive/negative heat anomalies poleward is equivalent to an equatorward eddy heat flux). This opposes the poleward heat transport from the mean ocean circulation. Warm tropical Indian and Indonesian Throughflow water feeds the poleward flowing eastern boundary current (Leeuwin Current) and the westward flowing South Equatorial Current which joins the poleward western boundary current (Agulhas Current). The net poleward heat transport across 18°S and 32°S has been estimated from inverse models as 1.27 and 0.87 PW, respectively [*Sloyan and Rintoul*, 2001], with 0.4 PW net heat loss to the atmosphere between these two sections. The net equatorward eddy heat transport may contribute to this 0.4 PW reduction in poleward heat transport across the subtropical gyre. *Morrow et al.* [2003] have estimated that 6 long-lived warm eddies generated in the Leeuwin Current region would contribute 0.04 PW in eddy heat transport. A more quantitative study including both warm and cold eddy fluxes is required to determine their role in the net heat, salt, tracer budgets, based on additional hydrographic data or models.

5. Conclusions

[18] In the southeast Indian Ocean, and to a lesser extent the southeast Atlantic, ocean eddies detected by mapped satellite altimetry data show a divergence: warm eddies tend to propagate westward and equatorward, cold eddies propagate westward and poleward. These eddies are large enough to be influenced by the β-effect, and their meridional drift is induced by the change in planetary and relative vorticity on the flanks of the eddy. These divergent pathways of warm and cold ocean eddies may have repercussions on the global heat, salt and tracer budgets. Further studies are required to quantify whether divergent eddy transport in the eastern boundary regions could provides a counter-balance to the poleward heat transport of the western boundary currents.

[19] **Acknowledgment.** This work was funded by the Programme Nationale d'Etudes Dynamique du Climat (PNEDC) in France.

References

Birol, F., and R. A. Morrow (2003), Separation of quasi-semiannual Rossby waves from the eastern boundary of the Indian Ocean, *J. Mar. Res.*, *61*, 707–723.

Boebel, O., J. Lutjeharms, C. Schmid, W. Zenk, T. Rossby, and C. Barron (2003), The Cape Cauldron: A regime of turbulent inter-ocean exchange, *Deep Sea Res. II*, *50*, 57–86.

Challenor, P. G., P. Cipollini, and D. Cromwell (2001), Use of the 3D Radon transform to examine the properties of oceanic Rossby waves, *J. Atmos. Oceanic Technol.*, *18*, 1558–1566.

Chassignet, E. P., and B. Cushman-Roisin (1991), On the influence of a lower layer on the propagation of nonlinear oceanic eddies, *J. Phys. Oceanogr.*, *21*, 939–957.

Chelton, D. B., and M. G. Schlax (1996), Global observations of oceanic Rossby waves, *Science*, *272*, 234–238.

Cushman-Roisin, B. (1994), *Introduction to Geophysical Fluid Dynamics*, Prentice-Hall, Upper Saddle River, N. J.

Cushman-Roisin, B., E. P. Chassignet, and B. Tang (1990), Westward motion of mesoscale eddies, *J. Phys. Oceanogr.*, *20*, 97–113.

de Ruijter, W. P. M., A. Biastoch, S. S. Drijfhout, J. R. E. Lutjeharms, R. P. Matano, T. Pichevin, P. J. van Leeuwen, and W. Weijer (1999), Indian-Atlantic inter-ocean exchange: Dynamics, estimation and impact, *J. Geophys. Res.*, *104*, 20,885–20,910.

Ducet, N., P. Y. Le Traon, and G. Reverdin (2000), Global high resolution mapping of ocean circulation from TOPEX/POSEIDON and ERS-1/2, *J. Geophys. Res.*, *105*, 19,477–19,498.

Fang, F., and R. Morrow (2003), Evolution and structure of Leeuwin Current eddies in 1995–2000, *Deep Sea Res. II*, *50*, 2245–2261.

Griffin, D. A., J. L. Wilkin, C. F. Chubb, A. F. Pearce, and N. Caputi (2001), Ocean currents and the larval phase of Australian western rock lobster, *Panulirus cygnus*, *Mar. Freshwater Res.*, *52*, 1187–1199.

Isern-Fontanet, J., E. Garcia-Ladona, and J. Font (2003), Identification of marine eddies from altimeter maps, *J. Atmos. Oceanic Technol.*, *20*, 772–778.

Josey, S. A., E. C. Kent, and P. K. Taylor (1999), New insights into the ocean heat budget closure problem from analysis of the SOC air-sea flux climatology, *J. Climate*, *12*, 2856–2880.

Le Traon, P. Y., and R. A. Morrow (2001), Ocean current and eddies, in *Satellite Altimetry and Earth Sciences*, edited by L.-L. Fu and A. Cazenave, pp. 171–215, Elsevier, New York.

Le Traon, P. Y., F. Nadal, and N. Ducet (1997), An improved mapping method of multi-satellite altimeter data, *J. Atmos. Oceanic Technol.*, *15*, 522–534.

McCartney, M. S. (1982), Subtropical recirculation of mode waters, *J. Mar. Res.*, *40*, suppl., 427–464.

Morrow, R., F. Fang, M. Fieux, and R. Molcard (2003), Anatomy of three warm-core Leeuwin current eddies, *Deep Sea Res. II*, *50*, 2229–2243.

Morrow, R., J.-R. Donguy, A. Chaigneau, and S. R. Rintoul (2004), Cold-core anomalies at the subantarctic front, south of Tasmania, *Deep Sea Res. I*, *51*, 1417–1440.

Sloyan, B. M., and S. R. Rintoul (2001), Circulation, renewal and modification of Antarctic mode and intermediate water, *J. Phys. Oceanogr.*, *31*, 1005–1030.

F. Birol, R. Morrow, and J. Sudre, Laboratoire d'Etudes en Géophysique et Océanographie Spatiales, 18 av. E. Belin, 31401 Toulouse Cedex 9, France. (rosemary.morrow@cnes.fr)

D. Griffin, Commonwealth Scientific and Industrial Research Organization Marine Research, P. O. Box 1538, Hobart, Tasmania 7001, Australia.